

Approximate total variation reconstruction of a wisdom tooth cross section from 2-dimensional X-ray projection images

Nicola Bagalà and Pekko Tuominen

INTRODUCTION

In this project we studied computing the inner structure of an object based on 2-dimensional X-ray projection images. The object in question was a wisdom tooth and our area of interest was the root of the tooth. The originally continuous problem was discretized and modeled to have the form

$$\mathbf{m} = A\mathbf{f} + \varepsilon \quad (1)$$

where the data \mathbf{m} and measurement matrix A are known, ε is an unknown noise term, and our goal is to extract information about \mathbf{f} . Problem (1) is a linear inverse problem containing an ill-conditioned matrix A , and a non-unique solution \mathbf{f} , making it ill-posed. For this reason we opted for approximate total variation as a regularization strategy in an attempt to solve (1); because of the large scale of the problem, we used the *Barzilai-Borwein* matrix-free gradient method in the arising minimization task. The goal of this project was, in the spirit of sparse angle tomography, to find a small amount of measurement angles that would still produce an acceptable reconstruction; acceptable meaning that the inner structure of the tooth's root could be seen.

METHODS AND MATERIALS

The data that we worked with consisted of 2-dimensional X-ray projection images of a wisdom tooth taken in the applied mathematics X-ray laboratory. We took images from 180 angles distributed evenly in the interval $[0^\circ, 180^\circ)$ and used subsets of this data to form reconstructions with limited data. Using the full data, filtered back projection (later FBP) was used for computing a ground truth that the other reconstruction were compared to. The reconstruction method used for the limited data was the approximate total variation regularization, implemented iteratively with the Barzilai-Borwein gradient descent method. In total variation we compute the solution to (1) as

$$T_\alpha(\mathbf{m}) = \arg \min_{\mathbf{f} \in \mathbb{R}^n} \{ \|\mathbf{A}\mathbf{f} - \mathbf{m}\|_2^2 + \alpha \|\mathbf{L}\mathbf{f}\|_p^p \} \quad (2)$$

where $\alpha > 0$ is the regularization parameter, $L \in \mathbb{R}^{n \times n}$ is the discretized differential operator and $p = 1$. Thus, we need to minimize

$$G(\mathbf{f}) = \|\mathbf{A}\mathbf{f} - \mathbf{m}\|_2^2 + \alpha \sum_{i,j} |\mathbf{f}_i - \mathbf{f}_j|,$$

where i and j index through all horizontally and vertically neighbouring pixel pairs. However, the presence of absolute values makes the functional G non differentiable; so, in order to be able to use gradient-based optimization, we introduce the following approximation:

$$|t| \approx |t|_\beta := \sqrt{t^2 + \beta}$$

where $\beta > 0$ is chosen to be small. Now we work on the continuously differentiable functional

$$G_\beta(\mathbf{f}) = \|\mathbf{A}\mathbf{f} - \mathbf{m}\|_2^2 + \alpha \sum_{i,j} |\mathbf{f}_i - \mathbf{f}_j|_\beta \quad (3)$$

and we can compute its gradient

$$\nabla G_\beta(\mathbf{f}) = \nabla \|\mathbf{A}\mathbf{f} - \mathbf{m}\|_2^2 + \alpha \nabla \left(\sum_{i,j} |\mathbf{f}_i - \mathbf{f}_j|_\beta \right).$$

The first part is given by

$$\nabla \|\mathbf{A}\mathbf{f} - \mathbf{m}\|_2^2 = 2A^T \mathbf{A}\mathbf{f} - 2A^T \mathbf{m};$$

since a pixel can have 2, 3 or 4 neighbours, for the second part the derivative with respect to $\mathbf{f}_{i,j}$ we have

$$\frac{\partial}{\partial \mathbf{f}_{i,j}} \|\mathbf{L}\mathbf{f}\|_1 = \frac{\mathbf{f}_{i,j} - \mathbf{f}_{i-1,j}}{((\mathbf{f}_{i,j} - \mathbf{f}_{i-1,j})^2 + \beta)} - \frac{\mathbf{f}_{i+1,j} - \mathbf{f}_{i,j}}{((\mathbf{f}_{i+1,j} - \mathbf{f}_{i,j})^2 + \beta)} + \frac{\mathbf{f}_{i,j} - \mathbf{f}_{i,j-1}}{((\mathbf{f}_{i,j} - \mathbf{f}_{i,j-1})^2 + \beta)} - \frac{\mathbf{f}_{i,j+1} - \mathbf{f}_{i,j}}{((\mathbf{f}_{i,j+1} - \mathbf{f}_{i,j})^2 + \beta)}$$

taking into account the terms that are defined.

The iteration of the Barzilai-Borwein method was started with a guess for both $\mathbf{f}^{(1)}$ and δ_1 , namely, $\mathbf{f}^{(1)} = 0$, and $\delta_1 = 10^{-4}$ and the next steps were found by means of the inductive formula

$$\mathbf{f}^{(\ell+1)} = \mathbf{f}^{(\ell)} - \delta_\ell \nabla G_\beta(\mathbf{f}^{(\ell)}),$$

with non-negativity constraint $\mathbf{f}^{(\ell+1)} = \max\{\mathbf{f}^{(\ell+1)}, 0\}$ and where $\delta_\ell = \frac{y_\ell^T y_\ell}{y_\ell^T g_\ell}$ and $y_\ell := \mathbf{f}^{(\ell)} - \mathbf{f}^{(\ell-1)}$, $g_\ell := \nabla G_\beta(\mathbf{f}^{(\ell)}) - \nabla G_\beta(\mathbf{f}^{(\ell-1)})$. As a halting criterion for the method we monitored 5 latest values of (3) and stopped when they were monotonically decreasing and the sum of their absolute differences became sufficiently small.

Matrix free implementation

Equations (1) and (2) contain a large matrix that needed to be replaced by an equivalent function for computational purposes. Applying matrix A to an image \mathbf{x} was replaced with $\mathcal{R}(\mathbf{x}, \theta)$, where \mathcal{R} stands for the *Radon transform* and θ specifies the measurement angles. We used MATLAB's built in function `radon.m`.

Parameter selection

As total variation is a sparsity promoting regularization strategy, we decided to use a sparsity based parameter choice for selecting the regularization parameter α , namely the S-curve method. This required a priori knowledge about the sparsity of the unknown solution. This information was found by computing the amount of essentially non-zero jumps in vertically and horizontally neighbouring pixel values in dental images taken from the Internet [2]. A good value for the parameter β in the implementation of Barzilai-Borwein was found empirically.

RESULTS

After testing that large α values did not produce good results, we computed a hundred reconstruction using $\alpha \in (0, 10]$ with logarithmic spacing and computed the jump ratio of each to produce Figure 1. The two constant lines are the jump ratio of the FBP and the mean jump ratio of the a priori information. In each case, the jump ratio was determined by first scaling the image values to the interval $[0, 1]$ and then computing the ratio of absolute pixel transitions that exceeded 0.05.

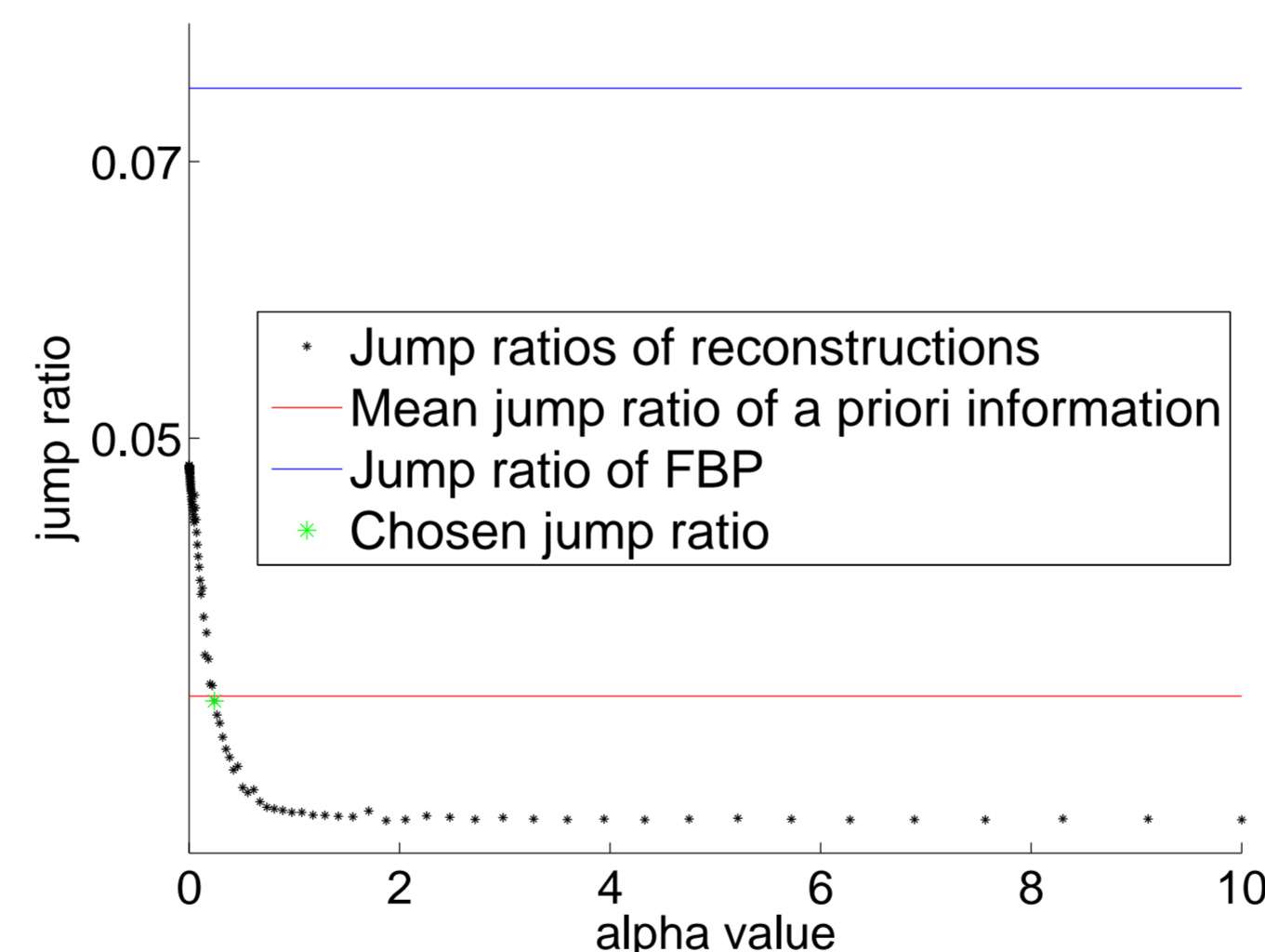


Figure 1: Jump ratios with different alpha values

We chose the α value as proposed in [1], namely $\alpha = 0.2420$. The corresponding total variation reconstruction using 12 projections is presented in Figure 2.

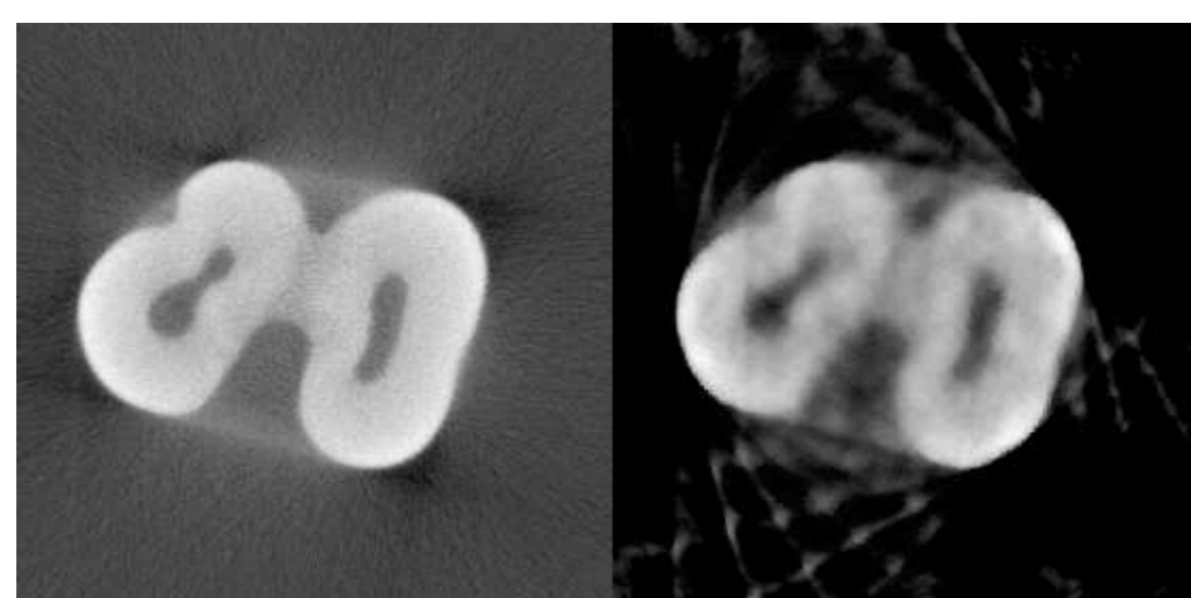


Figure 2: FBP (left) using full data and aTV (right) using 12 projections. The relative error is 17%.

In order to assess the accuracy of our automated parameter selection method, we compared the same reconstructions to the filtered back projection and chose the one with smallest relative error.

This reconstruction found by "cheating" is presented in Figure 3 with the FBP. Here, the chosen regularization parameter value was $\alpha = 3,8986$.

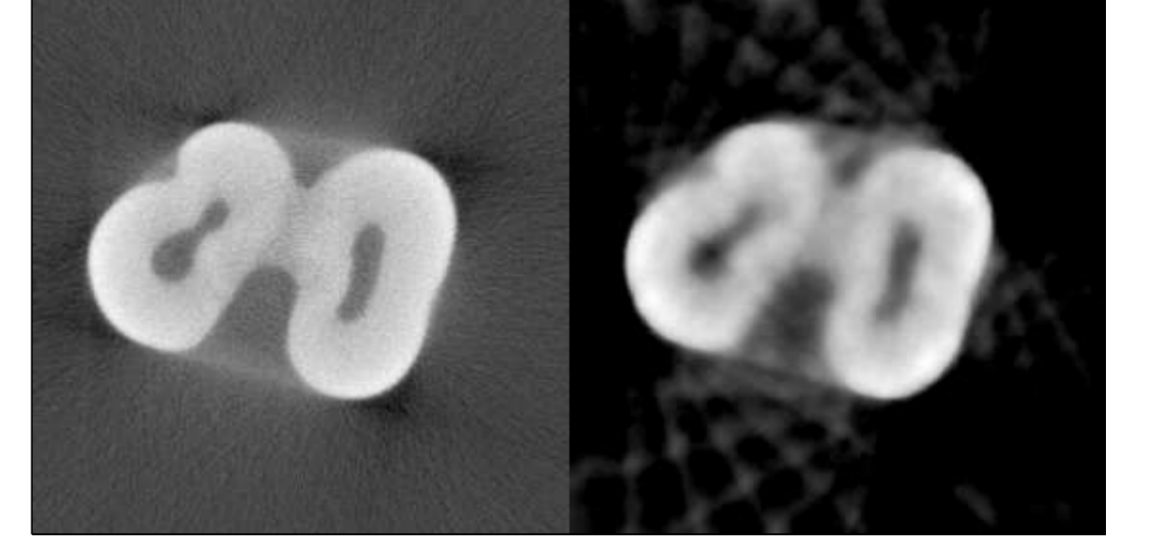


Figure 3: FBP (left) using full data and a limited data aTV reconstruction found by "cheating". The relative error is 14%.

The result of the filtered back projection using the limited data of 12 projection is illustrated in the middle of Figure 4. Its relative error w.r.t. the full data version is 51%.

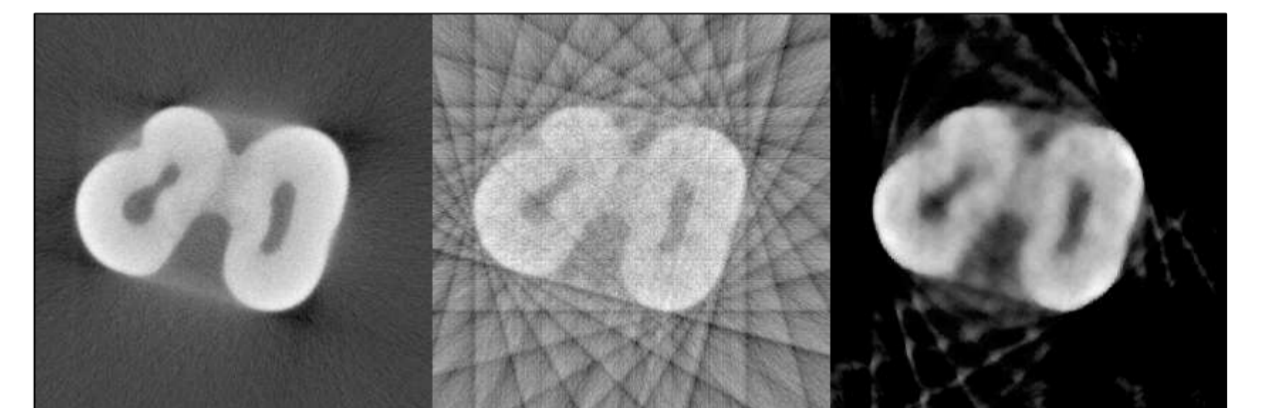


Figure 4: FBP with full data (left), FBP (center) and aTV (right) with 12 projections

The mentioned a priori images [2] are presented in Figure 5. Although they are not identical to the FBP image, they proved useful in selecting the regularization parameter.

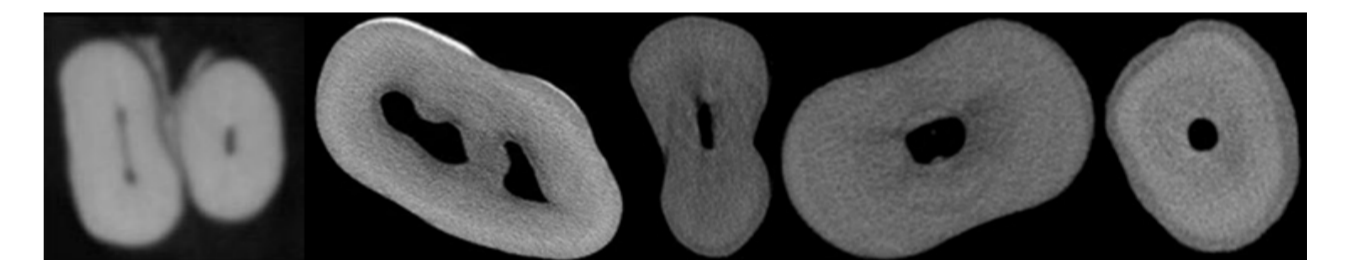


Figure 5: The dental images used as a priori information

The β and δ_1 values used in the Barzilai-Borwein optimization were chosen to be $\beta = 10^{-6}$ and $\delta_1 = 10^{-4}$.

DISCUSSION

The jump ratio of the FBP was not used in the parameter selection, it is displayed in figure 1 for comparison. As can be seen, its jump ratio differs from the ratio of the reconstructions. This makes sense, since aTV encourages sparsity. The amount of a priori images was quite small, namely five, but their mean sparsity level was such that it yielded a good parameter. The relative error of the corresponding aTV reconstruction using 12 projections was just 17%. The goodness of this reconstruction is backed up by the "erroneously" found optimal reconstruction whose relative error was 14%, so only three percent better. The outer structure of the tooth and the shape of its hollow inner structure can be seen quite clearly in our "legitimately" found reconstruction. Some empty space artefacts are present, but they do not obscure the structure of the tooth.

Total variation performed much better with limited data than the filtered back projection. The amount of artefacts is substantially higher in the FBP reconstruction when using only 12 projection images and the relative error is three times larger, namely 51%. We note that there are *measuring* artefacts in the FBP reconstruction with full data. One can clearly see e.g. the ring artefacts caused by sensitivity differences in the detectors pixels. In addition there are artefacts due to beam hardening and measurement geometry present in the data. It seems that there is hardly anything left of the ring artefacts in the total variation reconstruction. This is a good thing, since they are naturally an unwanted feature.

To conclude, approximate total variation provides a rather good reconstruction of the wisdom tooth cross section in the case of limited data, which the FBP technique does not handle as well.

References

- [1] Mueller J L and Siltanen S, *Linear and Nonlinear Inverse Problems with Practical Applications*, SIAM 2012.
- [2] <http://rootcanalanatomy.blogspot.fi/>